NEUROSCIENCE

*APOE*ε4 associates with microglial activation independently of Aβ plaques and tau tangles

João Pedro Ferrari-Souza[1,2]†, Firoza Z. Lussier[1,3]†, Douglas T. Leffa[1,4], Joseph Therriault[3], Cécile Tissot[1,3], Bruna Bellaver[1,2], Pâmela C. L. Ferreira[1], Maura Malpetti[5], Yi-Ting Wang[3], Guilherme Povala[1,2], Andréa L. Benedet[3,6], Nicholas J. Ashton[6,7,8], Mira Chamoun[3], Stijn Servaes[3], Gleb Bezgin[3,9], Min Su Kang[3,10,11], Jenna Stevenson[3], Nesrine Rahmouni[3], Vanessa Pallen[3], Nina Margherita Poltronetti[3], John T. O'Brien[5,12], James B. Rowe[5,13], Ann D. Cohen[1], Oscar L. Lopez[14], Dana L. Tudorascu[1], Thomas K. Karikari[1,6,15], William E. Klunk[1], Victor L. Villemagne[1], Jean-Paul Soucy[9], Serge Gauthier[3], Diogo O. Souza[2], Henrik Zetterberg[6,15,16,17,18], Kaj Blennow[6,15], Eduardo R. Zimmer[2,19,20], Pedro Rosa-Neto[3], Tharick A. Pascoal[1,14]*

Animal studies suggest that the apolipoprotein E ε4 (*APOE*ε4) allele is a culprit of early microglial activation in Alzheimer's disease (AD). Here, we tested the association between *APOE*ε4 status and microglial activation in living individuals across the aging and AD spectrum. We studied 118 individuals with positron emission tomography for amyloid-β (Aβ; [^{18}F]AZD4694), tau ([^{18}F]MK6240), and microglial activation ([^{11}C]PBR28). We found that *APOE*ε4 carriers presented increased microglial activation relative to noncarriers in early Braak stage regions within the medial temporal cortex accounting for Aβ and tau deposition. Furthermore, microglial activation mediated the Aβ-independent effects of *APOE*ε4 on tau accumulation, which was further associated with neurodegeneration and clinical impairment. The physiological distribution of *APOE* mRNA expression predicted the patterns of *APOE*ε4-related microglial activation in our population, suggesting that *APOE* gene expression may regulate the local vulnerability to neuroinflammation. Our results support that the *APOE*ε4 genotype exerts Aβ-independent effects on AD pathogenesis by activating microglia in brain regions associated with early tau deposition.

INTRODUCTION

Alzheimer's disease (AD) is a multifactorial disorder neuropathologically characterized by amyloid-β (Aβ) plaques and tau neurofibrillary tangles (*1*, *2*). Among the multiple pathogenic processes involved in AD etiology, neuroinflammation, commonly associated with microglial reactivity, has been increasingly recognized (*3*, *4*). Microglial activation plays a key role in the accumulation of AD hallmark proteinopathies, rather than being merely an epiphenomenon of their deposition (*3*, *4*). Specifically, recent observations from animal and human studies suggest that microglial activation precedes and may drive tau spread over the neocortex following a Braak stage–like pattern (*5*–*7*), from the medial temporal to association and primary sensory structures (*8*–*11*). Such microglial activation is synaptotoxic, affects brain connectivity, and predicts clinical decline (*12*, *13*). Aβ pathology can trigger microglial activation in AD (*14*–*16*), but Aβ plaques and activated microglia only partially overlap topographically in the human brain (*17*–*19*), and microglial activation may occur before demonstrable Aβ deposition (*3*).

The apolipoprotein E ε4 (*APOE*ε4) allele is a major genetic risk factor for sporadic AD (*20*–*23*). The link between *APOE*ε4 and Aβ deposition is an important factor leading to AD progression (*24*). However, recent animal studies suggest that the *APOE*ε4 genotype may also contribute to AD pathogenesis through Aβ-independent pathways by potentiating brain inflammation, tau accumulation, and neurodegeneration (*25*, *26*). Although robust experimental evidence indicates that the *APOE* genotype modulates microglial response in AD (*25*, *27*–*30*), it remains to be elucidated whether the

[1]Department of Psychiatry, University of Pittsburgh, Pittsburgh, PA, USA. [2]Graduate Program in Biological Sciences: Biochemistry, Universidade Federal do Rio Grande do Sul, Porto Alegre, RS, Brazil. [3]Translational Neuroimaging Laboratory, McGill University Research Centre for Studies in Aging, Alzheimer's Disease Research Unit, Douglas Research Institute, Le Centre intégré universitaire de santé et de services sociaux (CIUSSS) de l'Ouest-de-l'Île-de-Montréal; Department of Neurology and Neurosurgery, Psychiatry and Pharmacology and Therapeutics, McGill University, Montreal, QC, Canada. [4]ADHD Outpatient Program and Development Psychiatry Program, Hospital de Clínicas de Porto Alegre, Porto Alegre, RS, Brazil. [5]Department of Clinical Neurosciences, Cambridge University Hospitals NHS Trust, University of Cambridge, Cambridge, UK. [6]Department of Psychiatry and Neurochemistry, The Sahlgrenska Academy at the University of Gothenburg, Mölndal, Sweden. [7]Centre for Age-Related Medicine, Stavanger University Hospital, Stavanger, Norway. [8]Department of Old Age Psychiatry, Institute of Psychiatry, Psychology and Neuroscience, King's College London, London, UK. [9]Montreal Neurological Institute, McGill University, Montreal, QC, Canada. [10]Artificial Intelligence and Computational Neurosciences lab, Sunnybrook Research Institute, University of Toronto, Toronto, ON, Canada. [11]LC Campbell Cognitive Neurology Unit, Hurvitz Brain Sciences Program, Sunnybrook Research Institute, University of Toronto, Toronto, ON, Canada. [12]Department of Psychiatry, University of Cambridge, Cambridge, UK. [13]MRC Cognition and Brain Sciences Unit, University of Cambridge, Cambridge, UK. [14]Department of Neurology, University of Pittsburgh, Pittsburgh, PA, USA. [15]Clinical Neurochemistry Laboratory, Sahlgrenska University Hospital, Gothenburg, Sweden. [16]Department of Neurodegenerative Disease, UCL Queen Square Institute of Neurology, London, UK. [17]UK Dementia Research Institute at UCL, London, UK. [18]Hong Kong Center for Neurodegenerative Diseases, Hong Kong, China. [19]Department of Pharmacology, Universidade Federal do Rio Grande do Sul, Porto Alegre, RS, Brazil. [20]Graduate Program in Biological Sciences: Pharmacology and Therapeutics, Universidade Federal do Rio Grande do Sul, Porto Alegre, RS, Brazil.
*Corresponding author. Email: pascoalt@upmc.edu.
†These authors contributed equally to this work.

presence of the *APOE*ε4 allele is associated with microglial activation in the AD human brain. The characterization of this association in living individuals is critical to confirm the Aβ-independent detrimental effects of *APOE*ε4 on microglia homeostasis and to support the development of therapeutic strategies.

Using complementary positron emission tomography (PET) radiotracers for the topographical quantification of microglial activation, Aβ, and tau accumulation across the brain, we investigated the association between the *APOE*ε4 genotype, microglial activation, Aβ, and tau in a cohort of individuals across the aging and AD continuum. We hypothesized that *APOE*ε4 is associated with microglial activation independently of AD hallmark proteinopathies. We then tested whether microglial activation mediates the effects of *APOE*ε4 on tau accumulation, neurodegeneration, and clinical impairment. Postmortem data from the Allen Human Brain Atlas were used to test the link between regional levels of brain *APOE* gene expression and the distribution of microglial activation as a function of the *APOE*ε4 genotype.

RESULTS

Participants

We screened 606 people for the rs6971 polymorphism in the translocator protein (*TSPO*) gene. Of the 314 high-affinity binders, we studied 118 individuals that were across the aging and AD spectrum [79 cognitively unimpaired (CU), 23 with mild cognitive impairment (MCI), and 16 with AD dementia] with [^{18}F]AZD4694 Aβ PET, [^{18}F]MK6240 tau PET, [^{11}C]PBR28 microglial activation PET, and magnetic resonance imaging (MRI), as well as *APOE* genotyping (fig. S1). Demographic characteristics of the population are reported in Table 1. Information regarding the prevalence of *APOE* genotypes in our sample is described in table S1.

Table 1. Demographics and key characteristics of participants by clinical diagnosis. Continuous variables are presented as mean (SD). CU, cognitively unimpaired; MCI, mild cognitive impairment; AD, Alzheimer's disease; CDR-SB, clinical dementia rating scale sum of boxes; MMSE, mini-mental state examination; ROI, region of interest; SUVR, standardized uptake value ratio.

	CU	MCI	AD
No.	79	23	16
Age, years	72.3 (5.7)	73.0 (5.3)	70.1 (10.3)
Male, no. (%)	17 (21.5)	14 (60.9)	9 (56.3)
Education, years	15.2 (3.7)	15.5 (2.9)	13.6 (3.8)
*APOE*ε4 carrier, no. (%)	23 (29.1)	15 (65.2)	7 (43.8)
MMSE score	29.2 (1.0)	28.2 (1.6)	22.1 (5.9)
CDR-SB score	0.1 (0.2)	1.5 (0.8)	5.3 (2.5)
Global [^{18}F]AZD4694 SUVR	1.52 (0.43)	2.18 (0.58)	2.42 (0.54)
Braak I-II [^{18}F]MK6240 SUVR	0.94 (0.19)	1.38 (0.52)	1.60 (0.39)
Braak III-IV [^{18}F]MK6240 SUVR	0.96 (0.10)	1.28 (0.53)	2.19 (1.13)
Braak V-VI [^{18}F]MK6240 SUVR	0.98 (0.09)	1.16 (0.31)	2.05 (1.22)
Hippocampal volume, cm^3	3.45 (0.34)	3.18 (0.34)	2.95 (0.55)

*APOE*ε4 associates with microglial activation in the medial temporal cortex

To test the association between *APOE*ε4 status and [^{11}C]PBR28 microglial activation PET, we conducted linear regression analyses adjusting for age, sex, and clinical diagnosis. Voxel-wise regression analysis showed that *APOE*ε4 carriers had higher [^{11}C]PBR28 uptake relative to noncarriers mainly in medial temporal structures (transentorhinal, entorhinal, and hippocampal cortices), which are the regions corresponding to early Braak stages (Fig. 1, A and B). Regarding the spatial extent of the voxel-wise results, the association between the presence of the *APOE*ε4 allele and [^{11}C]PBR28 [standardized uptake value ratio (SUVR)] was predominantly observed in areas corresponding to Braak I (affecting 94.8% of this region), followed by Braak II (47.6%), Braak III (16.7%), Braak IV (13.1%), Braak V (2.5%), and Braak VI regions (1.0%; Fig. 1C). Similarly, in terms of the magnitude of the associations (β estimate), the relationship between *APOE*ε4 and [^{11}C]PBR28 uptake was progressively weaker from Braak I to VI, surviving Bonferroni correction for multiple comparisons only in Braak I and II regions [Braak I: β = 0.088; 95% confidence interval (CI), 0.044 to 0.133; $P < 0.001$; Braak II: β = 0.066; 95% CI, 0.020 to 0.111; $P = 0.005$; Fig. 1D]. Sensitivity analysis excluding individuals bearing the ε2 allele of the *APOE* gene showed similar findings (fig. S2). Results stratifying individuals according to the cognitive status are presented in fig. S3. In a subset of 42 individuals (33 CU, 6 with MCI, and 3 with AD dementia) with available clinical follow-up data (≥1 year after baseline), we tested the association of microglial activation with longitudinal neurodegeneration and clinical decline. Linear regression models accounting for age, sex, and clinical diagnosis revealed that higher [^{11}C]PBR28 SUVR in the brain regions vulnerable to *APOE*ε4 effects on microglial activation was associated with higher rates of longitudinal hippocampal atrophy (β = −0.293; 95% CI, −0.539 to −0.046; $P = 0.021$; fig. S4A) and clinical decline (β = 3.378; 95% CI, 1.783 to 4.974; $P < 0.001$; fig. S4B).

*APOE*ε4 associates with microglial activation even accounting for Aβ and tau biomarkers

We investigated the association between the *APOE*ε4 genotype and [^{11}C]PBR28 uptake accounting for AD hallmark proteinopathies using linear regression analysis. We observed a statistically significant association between the presence of the *APOE*ε4 allele and higher [^{11}C]PBR28 uptake in Braak I-II regions, accounting for global Aβ and local tau PET, as well as age, sex, and clinical diagnosis (β = 0.055; 95% CI, 0.010 to 0.100; $P = 0.018$; Table 2). Regarding AD proteinopathies effects in this regression model, we found that Braak I-II [^{11}C]PBR28 SUVR was significantly associated with local tau PET SUVR (β = 0.109; 95% CI, 0.031 to 0.187; $P = 0.006$; Table 2) but not with global Aβ PET SUVR (β = −0.030; 95% CI, −0.079 to 0.019; $P = 0.232$; Table 2). In a subgroup of 51 participants (31 CU, 12 with MCI, and 8 with AD dementia), we conducted sensitivity analyses accounting for cerebrospinal fluid (CSF) $A\beta_{1-42}$ and tau phosphorylated at threonine 181 ($p\text{-}tau_{181}$) instead of [^{18}F]AZD4694 Aβ PET and [^{18}F]MK6240 tau PET, respectively. Demographics for the subgroup of participants are presented in table S2. Similarly, we found that the presence of the *APOE*ε4 allele was significantly associated with higher [^{11}C]PBR28 SUVR in Braak I-II regions (β = 0.073; 95% CI, 0.005 to 0.140; $P = 0.035$; Table 3), which reinforces the cross-modality imaging results. In relation to the biomarkers for AD hallmark proteins, this model showed that Braak I-

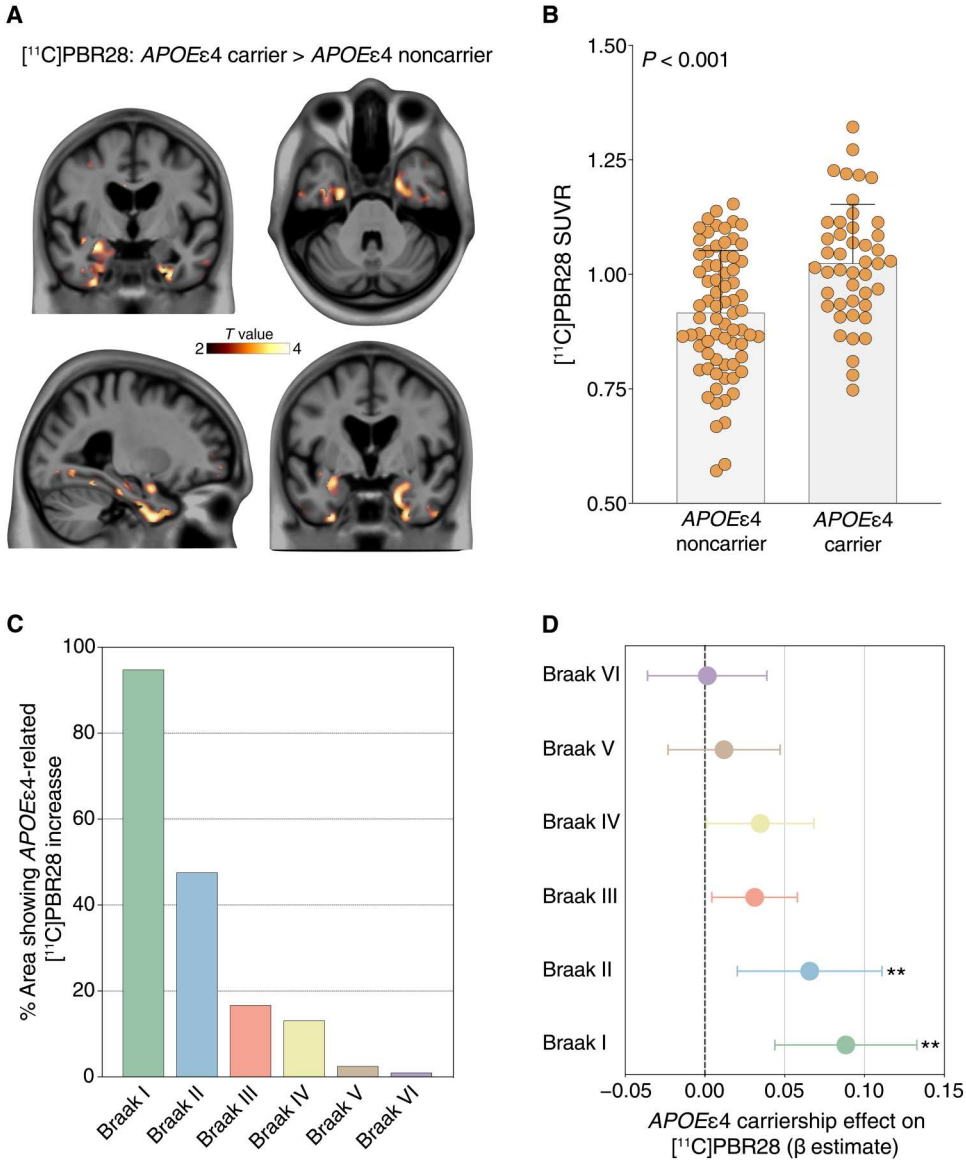

Fig. 1. *APOE*ε4 is associated with microglial activation in early Braak regions. (**A**) *T* map shows the result of voxel-wise linear regression testing the association of *APOE*ε4 carriage status (noncarrier or carrier) with [^{11}C]PBR28 SUVR accounting for age, sex, and clinical diagnosis [Cognitively unimpaired (CU), mild cognitive impairment (MCI) or Alzheimer's disease (AD)]. Results survived random field theory correction for multiple comparisons at $P < 0.05$. (**B**) Bars show the mean and SD of [^{11}C]PBR28 standardized uptake value ratio (SUVR) in *APOE*ε4 noncarriers and carriers. Imaging biomarker values were extracted from the peak *T* value cluster of the voxel-wise analysis (*T* value ≥ 4.7). *P* value indicates the result of regression analysis accounting for age, sex, and clinical diagnosis. (**C**) Bars represent the spatial extent of the *APOE*ε4-related microglia activation across Braak regions. Values were calculated by determining the percentage of voxels per Braak region having an association (*T* value > 2) between *APOE*ε4 and [^{11}C]PBR28 in the voxel-wise analysis. (**D**) β estimates with 95% confidence interval (CI) represent the strength of the regional association between *APOE*ε4 status and [^{11}C]PBR28 SUVR across Braak regions from region of interest (ROI)–based linear regressions. Models were adjusted for age, sex, and clinical diagnosis. Estimates that survived Bonferroni correction at $P < 0.05$ are indicated with a double asterisk.

II [^{11}C]PBR28 SUVR was significantly associated with CSF Aβ_{1-42} levels (β = 0.0001; 95% CI, 0.00001 to 0.0002; $P = 0.027$; Table 3) but not with CSF p-tau$_{181}$ levels (β = 0.0004; 95% CI, −0.0003 to 0.001; $P = 0.273$; Table 3). Exploratory analyses conducted across the six Braak regions supported that the investigated association of *APOE*ε4 with [^{11}C]PBR28 uptake was mainly confined to early Braak regions, either assessing AD hallmark proteins with imaging ([^{18}F]AZD4694 Aβ PET and [^{18}F]MK6240 tau PET; table S3) or fluid biomarkers (CSF Aβ_{1-42} and p-tau$_{181}$; table S4).

APOE gene expression resembles *APOE*ε4-related microglial activation patterns

We studied the topographical distribution of *APOE* mRNA in the postmortem brain of six CU individuals from the Allen Human Brain Atlas. We observed different *APOE* gene expression levels across Braak regions, which were progressively lower from Braak I to VI (Fig. 2A), suggesting that the cerebral levels of *APOE* gene expression partially follow Braak-like stages. In addition, linear regressions demonstrated that the regional patterns of Allen *APOE*

Table 2. Association between *APOE*ε4 and microglial activation accounting for Aβ positron emission tomography (PET) and tau PET. Aβ pathology was measured with global [^{18}F]AZD4694 standardized uptake value ratio (SUVR), microglial activation with Braak I-II [^{11}C]PBR28 SUVR, and tau pathology with Braak I-II [^{18}F]MK6240 SUVR. CU, cognitively unimpaired; MCI, mild cognitive impairment.

	β (95% CI)	*T* value	*P* value
Model: [^{11}C]PBR28 SUVR ~ *APOE*ε4 status + [^{18}F]AZD4694 SUVR + [^{18}F]MK6240 SUVR + age + sex + clinical diagnosis			
*APOE*ε4 carriership	0.055 (0.010 to 0.100)	2.404	0.018
[^{18}F]AZD4694 SUVR	−0.030 (−0.079 to 0.019)	−1.203	0.232
[^{18}F]MK6240 SUVR	0.109 (0.031 to 0.187)	2.779	0.006
Age	0.001 (−0.002 to 0.004)	0.631	0.530
Male	−0.015 (−0.061 to 0.031)	−0.656	0.513
Clinical diagnosis			
MCI	−0.064 (−0.129 to 0.001)	−1.954	0.053
AD	−0.071 (−0.151 to 0.009)	−1.758	0.082

Table 3. Sensitivity analysis testing the association of *APOE*ε4 with microglial activation accounting for cerebrospinal fluid (CSF) $A\beta_{1-42}$ and p-tau_{181}. Aβ pathology was measured with CSF $A\beta_{1-42}$, tau pathology with CSF p-tau_{181}, and microglial activation with Braak I-II [^{11}C]PBR28 standardized uptake value ratio (SUVR). p-tau_{181} = tau phosphorylated at threonine 181. MCI, mild cognitive impairment; AD, Alzheimer's disease.

	β (95% CI)	*T* value	*P* value
Model: [^{11}C]PBR28 SUVR ~ *APOE*ε4 status + CSF $A\beta_{1-42}$ + CSF p-tau_{181} + age + sex + clinical diagnosis			
*APOE*ε4 carriership	0.073 (0.005 to 0.140)	2.179	0.035
CSF $A\beta_{1-42}$	0.0001 (0.00001 to 0.0002)	2.298	0.027
CSF p-tau_{181}	0.0004 (−0.0003 to 0.001)	1.110	0.273
Age	0.007 (0.002 to 0.012)	2.799	0.008
Male	−0.013 (−0.077 to 0.051)	−0.422	0.675
Clinical diagnosis			
MCI	−0.011 (−0.099 to 0.077)	−0.252	0.802
AD	0.054 (−0.048 to 0.156)	1.062	0.294

mRNA expression across Braak regions predicted the topography and magnitude of *APOE*ε4 effects on [^{11}C]PBR28 uptake observed in our population (Fig. 2, B and C). By contrast, across non-Braak regions [i.e., Desikan-Killiany-Tourville (DKT)–based regions of interest (ROIs) not included in the Braak mask used in the present work], the regional patterns of *APOE* mRNA brain expression were not associated with *APOE*ε4 effects on [^{11}C]PBR28 uptake observed in our study population, neither in terms of topography ($P = 0.282$) nor in terms of magnitude ($P = 0.592$).

Microglial activation mediates the Aβ-independent effects of *APOE*ε4 on AD markers

We next used structural equation modeling to investigate the associations between *APOE*ε4, microglial activation, Aβ, tau, hippocampal volume, and clinical function [as measured with the clinical dementia rating scale sum of boxes (CDR-SB)]. In a model assessing microglial activation and tau pathology in medial temporal structures, we found that an increase in [^{11}C]PBR28 microglial activation uptake partially mediated the effects of *APOE*ε4 on higher tau PET uptake in Braak I-II regions independently of Aβ PET burden. The model also showed a separate pathway in which *APOE*ε4 effects on higher tau PET uptake occurred partially through higher Aβ PET load independently of microglial activation. Notably, both Aβ-independent and Aβ-dependent pathways leading to medial temporal tau pathology were further associated with lower hippocampal volume and, ultimately, higher severity of clinical impairment (Fig. 3 and table S5). This model fits the data well [$n = 118$, $X^2 = 7.141$, df = 5, $P = 0.210$, root mean square error of approximation (RMSEA) = 0.060, standardized root mean square residual (SRMR) = 0.023, comparative fit index (CFI) = 0.991]. A separate model assessing tau pathology and microglial activation in areas outside the medial temporal lobe is reported in fig. S5 and table S6.

DISCUSSION

In the current study, we observed that the presence of the *APOE*ε4 allele was associated with microglial activation in early Braak stage regions. This relationship persisted after accounting for AD hallmark proteinopathies. We also found that the brain distribution of *APOE* gene expression predicted the pattern of *APOE*ε4-related microglial activation observed in our study population. Last, we demonstrated that microglial activation partially mediated the *APOE*ε4 effects on regional tau accumulation through an Aβ-independent pathway, which was further associated with neurodegeneration and clinical impairment. Together, our findings support the hypothesis that *APOE*ε4 contributes to the early progression of AD via increased neuroinflammation.

The *APOE*ε4 genotype was associated with higher levels of microglial activation in living humans across the aging and AD continuum. Several recent investigations in animal models of AD support our findings. For example, the *APOE* genotype modulates microglial response in AD, with *APOE*ε4 being associated with multiple microglial-related detrimental downstream effects (e.g., protein aggregation, neurodegeneration, and dysfunctional immunometabolic response) (*25*, *27*–*30*). Further experiments showed that the *APOE*ε4 genotype associates with changes in the transcriptional profile of microglia from a homeostatic state to a disease-associated state across AD progression (*31*, *32*) and that the activation of microglial-related proteins [e.g., triggering receptor expressed on myeloid cells 2 (TREM2); (*33*–*36*)] is directly associated with ApoE signaling (*37*). This evidence raises the possibility that the mechanisms explaining the link between ApoE and microglial activation occur at the transcriptional level by the expression of microglia-specific genes such as *TREM2*. Together with our results showing that microglial activation in *APOE*ε4-vulnerable regions was associated with subsequent hippocampal atrophy and clinical deterioration, these findings suggest that the *APOE*ε4 genotype is associated with a disruption in microglia homeostasis in AD, promoting disease-associated microglia that plays a role in the development of the disease.

Our results showed an independent effect of *APOE*ε4 on medial temporal microglial activation leading to AD progression. Previous observations indicate that microglial activation may precede and drive tau propagation (*5*–*7*, *38*). Moreover, an investigation using

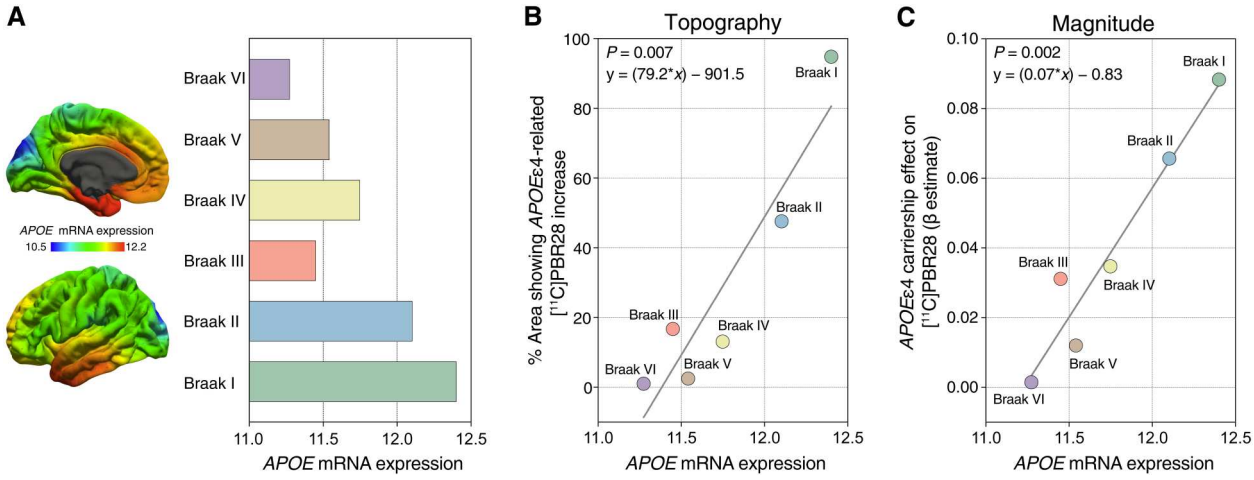

Fig. 2. The brain levels of *APOE* gene expression predict *APOE*ε4-related [^{11}C]PBR28 standardized uptake value ratio (SUVR) increase. (**A**) Brain map of the topographical distribution of *APOE* mRNA expression in six cognitively unimpaired (CU) individuals obtained from the Allen Human Brain Atlas (left). Average intensity values of *APOE* mRNA expression in each Braak region (right). (**B**) Regression analysis testing whether Allen brain *APOE* gene expression patterns predict the percentage of the area showing *APOE*ε4-related [^{11}C]PBR28 SUVR increase across Braak regions in our population. (**C**) Regression analysis testing whether the Allen brain *APOE* gene expression patterns predict the magnitude/strength of the association between *APOE*ε4 and [^{11}C]PBR28 uptake across Braak regions in our population.

the [^{11}C]PK11195 PET tracer found that microglial activation in the temporal lobe is associated with longitudinal cognitive decline more strongly than the [^{18}F]AV1451 tau PET tracer binding in patients presenting AD pathophysiology (*12*). We complemented these reports by demonstrating an Aβ-independent effect of *APOE*ε4 on early microglial activation in medial temporal structures, which, in turn, mediate tau accumulation that was further related to neurodegeneration and clinical decline. These results resonate with recent CSF biomarker evidence of neuroinflammation in adult *APOE*ε4 carriers who have not developed Aβ pathology yet (*39*). Our findings are also in line with animal model studies showing that the *APOE* genotype affects tau pathology and tau-mediated neurodegeneration independently of Aβ, with the *APOE*ε4 isoform having detrimental effects on both outcomes (*25*, *38*, *40*–*42*). In humans, the *APOE*ε4 allele has been associated with medial temporal atrophy (*43*–*46*). In addition, a recent study revealed that *APOE*ε4 carriers have higher tau PET uptake relative to noncarriers in the medial temporal lobe independently of Aβ, raising discussions about the importance of elucidating the biological underpinnings of this association (*47*). We built on these previous investigations suggesting that microglial activation is the mediator of the Aβ-independent effects of *APOE*ε4 on medial temporal tau deposition and brain atrophy, leading to dementia. Together, these results suggest that disease-modifying therapies targeting the interplay between ApoE and microglial activation have the potential to slow downstream AD progression.

We observed that cerebral *APOE* mRNA expression was more prominent in medial temporal structures and its levels hierarchically followed the Braak staging scheme. Although the Allen Human Brain Atlas is derived from younger adults without dementia, the *APOE* gene expression pattern was able to predict the topography and magnitude of the *APOE*ε4-related [^{11}C]PBR28 uptake increase in our cohort. It is well established that tau neurofibrillary tangles follow a stereotypical pattern of progression known as Braak stages, with tau tangles deposition starting in the medial temporal cortex (*8*–*11*). Microglial activation precedes and drives tau spread from the medial temporal lobe to the neocortex in a Braak-like pattern in AD models (*5*–*7*), although the mechanism associated with triggering microglial activation in medial temporal structures was not fully understood. Here, we showed, first, that *APOE*ε4 plays a role in triggering microglia activation in early Braak regions and, second, that a Braak-like pattern of *APOE* gene expression could shed light on the entire hierarchical progression of tau across these stages. These results indicate that microglia-mediated tau propagation in AD might be explained at least partially by the cerebral expression levels of ApoE4.

Strengths of the present work include the assessment of a well-characterized cohort with multiple PET radiotracers acquired on the same scanner, which allows high-quality topographical characterization of microglial activation, Aβ deposition, and tau accumulation using the best currently available technologies. Moreover, we screened a large sample of 606 individuals for the rs6971 polymorphism in the *TSPO* gene, and, consequently, we were able to include only high-affinity binders for the [^{11}C]PBR28 radiotracer, which increases the signal-to-noise ratio of the tracer and the reliability of our results.

Methodological limitations need to be acknowledged and considered to interpret our results. The [^{11}C]PBR28 radiotracer binds to the TSPO, which is a protein mainly expressed in the mitochondrial outer membrane of activated microglia (*3*). Thus, [^{11}C]PBR28 PET is considered an imaging biomarker of a general cerebral microglial activation state (*7*, *48*, *49*). However, it is recognized that microglia may acquire diverse phenotypes across disease progression (*3*), and this heterogeneity cannot be captured using the available human brain imaging technologies. Furthermore, it is possible that other cell types (e.g., astrocytes) also play a minor role in the TSPO PET signal (*3*, *50*–*53*). CSF measures have been suggested to detect Aβ and tau accumulation earlier than PET (*48*, *54*, *55*). We observed a consistent pattern for the association between *APOE*ε4 allele and [^{11}C]PBR28 SUVR when adjusting the models for PET imaging ([^{18}F]AZD4694 and [^{18}F]MK6240) and fluid (CSF $A\beta_{1-42}$ and p-tau_{181}) biomarkers; however, we cannot

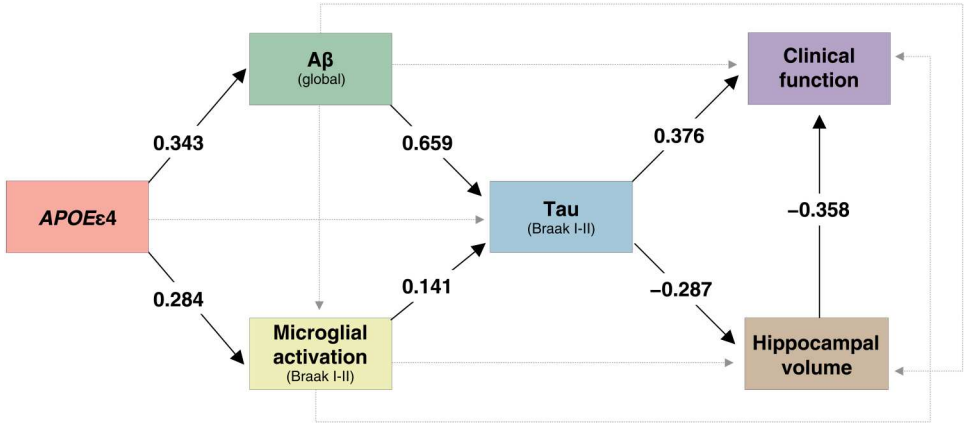

Fig. 3. *APOE*ε4 contributes to Alzheimer's disease (AD) progression independently of Aβ by activating microglia. The values presented in the figure are structural equation model β estimates testing the associations between *APOE*ε4 status, microglial activation positron emission tomography (PET), Aβ PET, tau PET, hippocampal volume, and clinical function. Given that the β estimates presented in the figure are standardized, the effects can be directly compared. Solid lines represent significant associations, whereas dashed lines represent nonsignificant effects. All associations were adjusted for age and sex. Associations involving hippocampal volume and clinical function were also adjusted for years of education. Aβ pathology was measured with global [^{18}F]AZD4694 standardized uptake value ratio (SUVR), microglial activation with Braak I-II [^{11}C]PBR28 SUVR, and tau pathology with Braak I-II [^{18}F]MK6240 SUVR. Clinical function was assessed with the clinical dementia rating scale sum of boxes (CDR-SB) score.

exclude a possible contribution of pre-plaque Aβ and tau conformations from our results. In medial temporal areas, while CSF $A\beta_{1-42}$ but not Aβ PET was directly associated with microglial activation, tau PET but not CSF p-tau_{181} was directly related to microglial activation. Several factors can play a role in these findings, such as that different aspects of AD pathophysiology are assessed with fluid (concentration of soluble proteins) and imaging (insoluble protein aggregation) markers (*56*). Additional studies are warranted to clarify the underpinnings of the relationships between imaging and fluid AD biomarkers with microglial activation. Although our statistical models were adjusted for sex, males were underrepresented in the CU group, which might compromise the generalizability of our results. Future studies using multiple longitudinal measures are needed to better evaluate the sequential relationship between neuroimaging biomarkers. Last, individuals included in our investigation were volunteers motivated to participate in a study about AD, which can be a source of self-selection bias.

In conclusion, our results support the existence of an Aβ-independent effect of *APOE*ε4 on AD progression through microglial activation, leading to tau accumulation, neurodegeneration, and eventually clinical impairment. These findings help to better understand the multifaceted role of the *APOE*ε4 genotype in the development of AD.

MATERIALS AND METHODS

Experimental design

The main objective of the present study was to test the association between the presence of the *APOE*ε4 allele and brain levels of microglial activation. We hypothesized that *APOE*ε4 is associated with microglial activation in early Braak regions independently of Aβ and tau pathologies. Furthermore, we aimed to assess whether microglial activation mediates the association between *APOE*ε4 and AD markers. Participants from the community or outpatients at the McGill University Research Centre for Studies in Aging were enrolled in the Translational Biomarkers in Aging and Dementia study (https://triad.tnl-mcgill.com). Participants were required to have adequate visual and auditory capacities for neuropsychological assessment, as well as the ability to speak English or French. In addition, individuals were not enrolled if they had active substance abuse, major surgery, recent head trauma, neuroimaging contraindication, simultaneously being enrolled in other studies, and untreated neurological, psychiatric, or systemic conditions. This study was approved by the Douglas Mental Health University Institute Research Ethics Board and the Montreal Neurological Institute (MNI) PET working committee, and all participants provided written informed consent.

Participants

Of the 606 individuals screened for the rs6971 polymorphism in the *TSPO* gene, we studied 118 individuals with high-affinity binding aged 52 to 87 years (79 CU, 23 with MCI, and 16 with AD dementia). At the same time point, all participants had PET for Aβ ([^{18}F]AZD4694), tau tangles ([^{18}F]MK6240), and microglial activation ([^{11}C]PBR28), as well as MRI and *APOE* genotyping. Two individuals that had [^{11}C]PBR28 or [^{18}F]MK6240 SUVR values of 3 SDs above the mean of the population were considered outliers as defined a priori and excluded from the analyses. A flowchart describing the selection of study participants is reported in fig. S1. Participants underwent detailed neuropsychological assessments, including mini-mental state examination and CDR. CU individuals had no objective cognitive impairment and a global CDR score of 0. MCI patients had subjective and objective cognitive impairment, preserved activities of daily living, and a global CDR score of 0.5 (*57*). Mild-to-moderate AD dementia patients had a global CDR score between 0.5 and 2 and met the National Institute on Aging and the Alzheimer's Association criteria for probable AD (*58*). We analyzed all the individuals with complete data, and no power analysis was performed before the study. Note that the sample size of the present work is similar to the largest previous TSPO PET studies across the AD spectrum (*7*, *59*–*61*).

Genetic data

[^{11}C]PBR28 binding affinity is influenced by a common polymorphism (rs6971) in the *TSPO* gene (www.ncbi.nlm.nih.gov/snp/rs6971). To increase the reliability of our results, we genotyped 606 participants for the rs6971 polymorphism before imaging, and we only included high-affinity binders (*7*). Note that this polymorphism is a methodological caveat and does not affect TSPO levels, glial activity, or AD pathological changes (*53*). Moreover, participants were genotyped for the *APOE* gene using the polymerase chain reaction amplification technique, followed by restriction enzyme digestion, standard gel resolution, and visualization processes (*62*).

Brain imaging

T1-weighted MRIs were acquired at the MNI using a 3T Siemens Magnetom. We used the magnetization prepared rapid acquisition gradient echo MRI (repetition time, 2300 ms; echo time, 2.96 ms) sequence to obtain high-resolution structural images of the whole brain (9° flip angle, coronal orientation perpendicular to the double spin echo sequence, 1 mm–by–1 mm in-plane resolution of 1 mm slab thickness) (*63*). Aβ PET with [^{18}F]AZD4694 (40 to 70 min after injection), tau PET with [^{18}F]MK-6240 (90 to 110 min after injection), and microglial activation TSPO PET with [^{11}C]PBR28 (60 to 90 min after injection) were acquired at the MNI using a Siemens High Resolution Research Tomograph. PET scans were reconstructed using the ordered subset expectation maximization algorithm on a four-dimensional volume with three frames (3 × 600 s) for [^{18}F]AZD4694 PET (*64*), four frames (4 × 300 s) for [^{18}F]MK-6240 PET (*64*), and six frames (6 × 300 s) for [^{11}C]PBR28 PET (*7*). Then, attenuation correction was performed using a 6-min transmission scan with a rotating ^{137}Cs point source. Furthermore, PET images were corrected for motion, dead time, decay, and scattered and random coincidences. Following an in-house pipeline, T1-weighted MRIs were corrected for nonuniformity and field distortion. Subsequently, linear coregistration and nonlinear spatial normalization for the Alzheimer's Disease Neuroimaging Initiative (ADNI) template were performed through linear and nonlinear transformation in two main steps: (i) PET registration to the correspondent T1-weighted MRI and (ii) T1-weighted MRI registration to the ADNI reference space. PET images were spatially smoothed to achieve a final resolution of 8-mm full width at half maximum. SUVRs were calculated using the whole cerebellum gray matter for [^{18}F]AZD4694 Aβ PET (*65*) and [^{11}C]PBR28 microglial activation PET (*7*) and the inferior cerebellum gray matter for [^{18}F]MK-6240 tau PET (*66*). The DKT atlas was used to determine the ROIs (*67*). A global Aβ PET SUVR was estimated from the precuneus, prefrontal, orbitofrontal, parietal, temporal, and cingulate cortices (*68*). On the basis of postmortem observations (*8*, *9*) and PET studies (*66*, *69*), PET Braak-like stages were calculated from brain regions corresponding to the Braak stages of tau neurofibrillary tangle accumulation: Braak I (transentorhinal), Braak II (entorhinal and hippocampus), Braak III (amygdala, parahippocampal gyrus, fusiform gyrus, and lingual gyrus), Braak IV (insula, inferior temporal, lateral temporal, posterior cingulate, and inferior parietal), Braak V (orbitofrontal, superior temporal, inferior frontal, cuneus, anterior cingulate, supramarginal gyrus, lateral occipital, precuneus, superior parietal, superior frontal, and rostro medial frontal), and Braak VI (paracentral, postcentral, precentral, and pericalcarine) (*66*, *70*). A representation of the Braak-like regions used in our analysis is shown in fig. S6. Hippocampal volume was adjusted for total intracranial volume using MRI data from CU individuals (*71*).

The Allen Human Brain Atlas (www.brain-map.org) (*72*) was used to obtain information regarding *APOE* gene expression in the brain. In brief, microarray was used to calculate mRNA expression intensity values on 3702 samples from six healthy human postmortem brains [four males, mean age = 42.5 (13.4) years, postmortem delay = 20.6 (7) hours]. The *APOE* mRNA brain expression maps were derived from a Gaussian process (*73*) and downloaded from www.meduniwien.ac.at/neuroimaging/mRNA.html.

CSF measurements

A subgroup of 51 individuals had CSF $A\beta_{1–42}$ and p-tau_{181} quantified using the LUMIPULSE G1200 instrument (Fujirebio) at the Clinical Neurochemistry Laboratory, University of Gothenburg, Mölndal, Sweden (*74*).

Statistical analysis

Analyses were performed in the R software (version 4.0.2, www.r-project.org/). Neuroimaging analyses were conducted using "RMINC" (*75*), an imaging package that allows the integration of voxel-based statistics into the R statistical environment. Voxel-wise and ROI-based linear regressions tested the association between *APOE*ε4 status (noncarrier or carrier) and microglial activation indexed by the [^{11}C]PBR28 SUVR adjusting for age, sex, and clinical diagnosis (CU, MCI, or AD). To further investigate whether this association was independent of AD hallmark proteins, ROI-based models were also adjusted for Aβ ([^{18}F]AZD4694 PET or CSF $A\beta_{1–42}$) and tau ([^{18}F]MK-6240 PET or CSF p-tau_{181}) biomarkers. Multiple comparisons correction at $P < 0.05$ was performed using random field theory for voxel-wise analysis and Bonferroni method for ROI-based analysis when appropriate. Linear regressions also assessed the association of [^{11}C]PBR28 SUVR with annual changes in hippocampal volume and CDR-SB score. We calculated the percentage of voxels in each Braak region showing an association (T value > 2) between the *APOE*ε4 genotype and [^{11}C]PBR28 SUVR in the aforementioned voxel-wise analysis. Regression analysis tested whether the *APOE* mRNA expression intensity predicted the topography and magnitude of *APOE*ε4-related [^{11}C]PBR28 SUVR increase across Braak regions. Structural equation modeling, R package "lavaan" (*76*), was used to test the associations between *APOE*ε4 status, microglial activation, Aβ, tau, hippocampal volume, and clinical function (as measured with CDR-SB). All the associations in the model were adjusted for age and sex; associations involving hippocampal volume and clinical deterioration were further adjusted for years of education. Structural equation model was judged as having a good fit as follows: CFI > 0.97 (acceptable, 0.95 to 0.97), RMSEA < 0.05 (acceptable, 0.05 to 0.08), and SRMR < 0.05 (acceptable, 0.05 to 0.10) (*77*, *78*). Statistical significance of parameters estimates from the structural equation model was tested using bootstrapping with 1000 permutations. For all analyses, two-tailed P values < 0.05 were considered statistically significant.

Supplementary Materials

This PDF file includes:

Figs. S1 to S6

Tables S1 to S6

View/request a protocol for this paper from *Bio-protocol*.

REFERENCES AND NOTES

1. J. C. Polanco, C. Li, L. G. Bodea, R. Martinez-Marmol, F. A. Meunier, J. Gotz, Amyloid-β and tau complexity—Towards improved biomarkers and targeted therapies. *Nat. Rev. Neurol.* **14**, 22–39 (2018).
2. D. S. Knopman, H. Amieva, R. C. Petersen, G. Chetelat, D. M. Holtzman, B. T. Hyman, R. A. Nixon, D. T. Jones, Alzheimer disease. *Nat. Rev. Dis. Primers.* **7**, 33 (2021).
3. F. Leng, P. Edison, Neuroinflammation and microglial activation in Alzheimer disease: Where do we go from here? *Nat. Rev. Neurol.* **17**, 157–172 (2021).
4. M. T. Heneka, M. J. Carson, J. El Khoury, G. E. Landreth, F. Brosseron, D. L. Feinstein, A. H. Jacobs, T. Wyss-Coray, J. Vitorica, R. M. Ransohoff, K. Herrup, S. A. Frautschy, B. Finsen, G. C. Brown, A. Verkhratsky, K. Yamanaka, J. Koistinaho, E. Latz, A. Halle, G. C. Petzold, T. Town, D. Morgan, M. L. Shinohara, V. H. Perry, C. Holmes, N. G. Bazan, D. J. Brooks, S. Hunot, B. Joseph, N. Deigendesch, O. Garaschuk, E. Boddeke, C. A. Dinarello, J. C. Breitner, G. M. Cole, D. T. Golenbock, M. P. Kummer, Neuroinflammation in Alzheimer's disease. *Lancet Neurol.* **14**, 388–405 (2015).
5. C. Ising, C. Venegas, S. Zhang, H. Scheiblich, S. V. Schmidt, A. Vieira-Saecker, S. Schwartz, S. Albasset, R. M. McManus, D. Tejera, A. Griep, F. Santarelli, F. Brosseron, S. Opitz, J. Stunden, M. Merten, R. Kayed, D. T. Golenbock, D. Blum, E. Latz, L. Buee, M. T. Heneka, NLRP3 inflammasome activation drives tau pathology. *Nature* **575**, 669–673 (2019).
6. S. C. Hopp, Y. Lin, D. Oakley, A. D. Roe, S. L. DeVos, D. Hanlon, B. T. Hyman, The role of microglia in processing and spreading of bioactive tau seeds in Alzheimer's disease. *J. Neuroinflammation* **15**, 269 (2018).
7. T. A. Pascoal, A. L. Benedet, N. J. Ashton, M. S. Kang, J. Therriault, M. Chamoun, M. Savard, F. Z. Lussier, C. Tissot, T. K. Karikari, J. Ottoy, S. Mathotaarachchi, J. Stevenson, G. Massarweh, M. Schöll, M. J. de Leon, J. P. Soucy, P. Edison, K. Blennow, H. Zetterberg, S. Gauthier, P. Rosa-Neto, Microglial activation and tau propagate jointly across Braak stages. *Nat. Med.* **27**, 1592–1599 (2021).
8. H. Braak, E. Braak, Neuropathological stageing of Alzheimer-related changes. *Acta Neuropathol.* **82**, 239–259 (1991).
9. H. Braak, E. Braak, Frequency of stages of Alzheimer-related lesions in different age categories. *Neurobiol. Aging* **18**, 351–357 (1997).
10. H. Braak, I. Alafuzoff, T. Arzberger, H. Kretzschmar, K. Del Tredici, Staging of Alzheimer disease-associated neurofibrillary pathology using paraffin sections and immunocytochemistry. *Acta Neuropathol.* **112**, 389–404 (2006).
11. H. Braak, D. R. Thal, E. Ghebremedhin, K. Del Tredici, Stages of the pathologic process in Alzheimer disease: Age categories from 1 to 100 years. *J. Neuropathol. Exp. Neurol.* **70**, 960–969 (2011).
12. M. Malpetti, R. A. Kievit, L. Passamonti, P. S. Jones, K. A. Tsvetanov, T. Rittman, E. Mak, N. Nicastro, W. R. Bevan-Jones, L. Su, Y. T. Hong, T. D. Fryer, F. I. Aigbirhio, J. T. O'Brien, J. B. Rowe, Microglial activation and tau burden predict cognitive decline in Alzheimer's disease. *Brain* **143**, 1588–1602 (2020).
13. L. Passamonti, K. A. Tsvetanov, P. S. Jones, W. R. Bevan-Jones, R. Arnold, R. J. Borchert, E. Mak, L. Su, J. T. O'Brien, J. B. Rowe, Neuroinflammation and functional connectivity in Alzheimer's disease: Interactive influences on cognitive performance. *J. Neurosci.* **39**, 7218–7226 (2019).
14. A. Hayes, U. Thaker, T. Iwatsubo, S. M. Pickering-Brown, D. M. A. Mann, Pathological relationships between microglial cell activity and tau and amyloid beta protein in patients with Alzheimer's disease. *Neurosci. Lett.* **331**, 171–174 (2002).
15. M. Kitazawa, T. R. Yamasaki, F. M. LaFerla, Microglia as a potential bridge between the amyloid β-peptide and tau. *Ann. N. Y. Acad. Sci.* **1035**, 85–103 (2004).
16. P. L. McGeer, E. G. McGeer, The amyloid cascade-inflammatory hypothesis of Alzheimer disease: Implications for therapy. *Acta Neuropathol.* **126**, 479–497 (2013).
17. A. Serrano-Pozo, M. L. Mielke, T. Gomez-Isla, R. A. Betensky, J. H. Growdon, M. P. Frosch, B. T. Hyman, Reactive glia not only associates with plaques but also parallels tangles in Alzheimer's disease. *Am. J. Pathol.* **179**, 1373–1384 (2011).
18. P. Parbo, R. Ismail, K. V. Hansen, A. Amidi, F. H. Marup, H. Gottrup, H. Braendgaard, B. O. Eriksson, S. F. Eskildsen, T. E. Lund, A. Tietze, P. Edison, N. Pavese, M. G. Stokholm, P. Borghammer, R. Hinz, J. Aanerud, D. J. Brooks, Brain inflammation accompanies amyloid in the majority of mild cognitive impairment cases due to Alzheimer's disease. *Brain* **140**, 2002–2011 (2017).
19. M. Dani, M. Wood, R. Mizoguchi, Z. Fan, Z. Walker, R. Morgan, R. Hinz, M. Biju, T. Kuruvilla, D. J. Brooks, P. Edison, Microglial activation correlates in vivo with both tau and amyloid in Alzheimer's disease. *Brain* **141**, 2740–2754 (2018).
20. L. A. Farrer, L. A. Cupples, J. L. Haines, B. Hyman, W. A. Kukull, R. Mayeux, R. H. Myers, M. A. Pericak-Vance, N. Risch, C. M. van Duijn, Effects of age, sex, and ethnicity on the association between apolipoprotein E genotype and Alzheimer disease. A meta-analysis. APOE and Alzheimer Disease Meta Analysis Consortium. *JAMA* **278**, 1349–1356 (1997).
21. E. Genin, D. Hannequin, D. Wallon, K. Sleegers, M. Hiltunen, O. Combarros, M. J. Bullido, S. Engelborghs, P. De Deyn, C. Berr, F. Pasquier, B. Dubois, G. Tognoni, N. Fiévet, N. Brouwers, K. Bettens, B. Arosio, E. Coto, M. Del Zompo, I. Mateo, J. Epelbaum, A. Frank-Garcia, S. Helisalmi, E. Porcellini, A. Pilotto, P. Forti, R. Ferri, E. Scarpini, G. Siciliano, V. Solfrizzi, S. Sorbi, G. Spalletta, F. Valdivieso, S. Vepsäläinen, V. Alvarez, P. Bosco, M. Mancuso, F. Panza, B. Nacmias, P. Bossù, O. Hanon, P. Piccardi, G. Annoni, D. Seripa, D. Galimberti, F. Licastro, H. Soininen, J.-F. Dartigues, M. I. Kamboh, C. Van Broeckhoven, J. C. Lambert, P. Amouyel, D. Campion, APOE and Alzheimer disease: A major gene with semi-dominant inheritance. *Mol. Psychiatry* **16**, 903–907 (2011).
22. J. C. Lambert, C. A. Ibrahim-Verbaas, D. Harold, A. C. Naj, R. Sims, C. Bellenguez, A. L. DeStafano, J. C. Bis, G. W. Beecham, B. Grenier-Boley, G. Russo, T. A. Thorton-Wells, N. Jones, A. V. Smith, V. Chouraki, C. Thomas, M. A. Ikram, D. Zelenika, B. N. Vardarajan, Y. Kamatani, C. F. Lin, A. Gerrish, H. Schmidt, B. Kunkle, M. L. Dunstan, A. Ruiz, M. T. Bihoreau, S. H. Choi, C. Reitz, F. Pasquier, C. Cruchaga, D. Craig, N. Amin, C. Berr, O. L. Lopez, P. L. De Jager, V. Deramecourt, J. A. Johnston, D. Evans, S. Lovestone, L. Letenneur, F. J. Moron, D. C. Rubinsztein, G. Eiriksdottir, K. Sleegers, A. M. Goate, N. Fiévet, M. W. Huentelman, M. Gill, K. Brown, M. I. Kamboh, L. Keller, P. Barberger-Gateau, B. McGuiness, E. B. Larson, R. Green, A. J. Myers, C. Dufouil, S. Todd, D. Wallon, S. Love, E. Rogaeva, J. Gallacher, P. St George-Hyslop, J. Clarimon, A. Lleo, A. Bayer, D. W. Tsuang, L. Yu, M. Tsolaki, P. Bossù, G. Spalletta, P. Proitsi, J. Collinge, S. Sorbi, F. Sanchez-Garcia, N. C. Fox, J. Hardy, M. C. D. Naranjo, P. Bosco, R. Clarke, C. Brayne, D. Galimberti, M. Mancuso, F. Matthews; European Alzheimer's Disease Initiative (EADI); Genetic and Environmental Risk in Alzheimer's Disease; Alzheimer's Disease Genetic Consortium; Cohorts for Heart and Aging Research in Genomic Epidemiology, S. Moebus, P. Mecocci, M. Del Zompo, W. Maier, H. Hampel, A. Pilotto, M. Bullido, F. Panza, P. Caffarra, B. Nacmias, J. R. Gilbert, M. Mayhaus, L. Lannefelt, H. Hakonarson, S. Pichler, M. M. Carrasquillo, M. Ingelsson, D. Beekly, V. Alvarez, F. Zou, O. Valladares, S. G. Younkin, E. Coto, K. L. Hamilton-Nelson, W. Gu, C. Razquin, P. Pastor, I. Mateo, M. J. Owen, K. M. Faber, P. V. Jonsson, O. Combarros, M. C. O'Donovan, L. B. Cantwell, H. Soininen, D. Blacker, S. Mead, T. H. Mosley Jr., D. A. Bennett, T. B. Harris, L. Fratiglioni, C. Holmes, R. F. de Bruijn, P. Passmore, T. J. Montine, K. Bettens, J. I. Rotter, A. Brice, K. Morgan, T. M. Foroud, W. A. Kukull, D. Hannequin, J. F. Powell, M. A. Nalls, K. Ritchie, K. L. Lunetta, J. S. Kauwe, E. Boerwinkle, M. Riemenschneider, M. Boada, M. Hiltuenen, E. R. Martin, R. Schmidt, D. Rujescu, L. S. Wang, J. F. Dartigues, R. Mayeux, C. Tzourio, A. Hofman, M. M. Nöthen, C. Graff, B. M. Psaty, L. Jones, J. L. Haines, P. A. Holmans, M. Lathrop, M. A. Pericak-Vance, L. J. Launer, L. A. Farrer, C. M. van Duijn, C. Van Broeckhoven, V. Moskvina, S. Seshadri, J. Williams, G. D. Schellenberg, P. Amouyel, Meta-analysis of 74,046 individuals identifies 11 new susceptibility loci for Alzheimer's disease. *Nat. Genet.* **45**, 1452–1458 (2013).
23. E. H. Corder, A. M. Saunders, W. J. Strittmatter, D. E. Schmechel, P. C. Gaskell, G. W. Small, A. D. Roses, J. L. Haines, M. A. Pericak-Vance, Gene dose of apolipoprotein E type 4 allele and the risk of Alzheimer's disease in late onset families. *Science* **261**, 921–923 (1993).
24. D. M. Holtzman, J. Herz, G. Bu, Apolipoprotein E and apolipoprotein E receptors: Normal biology and roles in Alzheimer disease. *Cold Spring Harb. Perspect. Med.* **2**, a006312 (2012).
25. Y. Shi, K. Yamada, S. A. Liddelow, S. T. Smith, L. Zhao, W. Luo, R. M. Tsai, S. Spina, L. T. Grinberg, J. C. Rojas, G. Gallardo, K. Wang, J. Roh, G. Robinson, M. B. Finn, H. Jiang, P. M. Sullivan, C. Baufeld, M. W. Wood, C. Sutphen, L. McCue, C. Xiong, J. L. Del-Aguila, J. C. Morris, C. Cruchaga; Alzheimer's Disease Neuroimaging Initiative, A. M. Fagan, B. L. Miller, A. L. Boxer, W. W. Seeley, O. Butovsky, B. A. Barres, S. M. Paul, D. M. Holtzman, ApoE4 markedly exacerbates tau-mediated neurodegeneration in a mouse model of tauopathy. *Nature* **549**, 523–527 (2017).
26. Y. Yamazaki, N. Zhao, T. R. Caulfield, C. C. Liu, G. Bu, Apolipoprotein E and Alzheimer disease: Pathobiology and targeting strategies. *Nat. Rev. Neurol.* **15**, 501–518 (2019).
27. C. D. Keene, E. Cudaback, X. Li, K. S. Montine, T. J. Montine, Apolipoprotein E isoforms and regulation of the innate immune response in brain of patients with Alzheimer's disease. *Curr. Opin. Neurobiol.* **21**, 920–928 (2011).
28. Y.-T. Lin, J. Seo, F. Gao, H. M. Feldman, H.-L. Wen, J. Penney, H. P. Cam, E. Gjoneska, W. K. Raja, J. Cheng, R. Rueda, O. Kritskiy, F. Abdurrob, Z. Peng, B. Milo, C. J. Yu, S. Elmsaouri, D. Dey, T. Ko, B. A. Yankner, L.-H. Tsai, APOE4 causes widespread molecular and cellular alterations associated with Alzheimer's disease phenotypes in human iPSC-derived brain cell types. *Neuron* **98**, 1141–1154 e7 (2018).
29. G. A. Rodriguez, L. M. Tai, M. J. LaDu, G. W. Rebeck, Human APOE4 increases microglia reactivity at Aβ plaques in a mouse model of Aβ deposition. *J. Neuroinflammation* **11**, 111 (2014).
30. S. Lee, N. A. Devanney, L. R. Golden, C. T. Smith, J. L. Schwarz, A. E. Walsh, H. A. Clarke, D. S. Goulding, E. J. Allenger, G. Morillo-Segovia, C. M. Friday, A. A. Gorman, T. R. Hawkinson, S. M. MacLean, H. C. Williams, R. C. Sun, J. M. Morganti, L. A. Johnson, *APOE* modulates

microglial immunometabolism in response to age, amyloid pathology, and inflammatory challenge. bioRxiv 2022.2005.2017.492361 (2022).
31. H. Keren-Shaul, A. Spinrad, A. Weiner, O. Matcovitch-Natan, R. Dvir-Szternfeld, T. K. Ulland, E. David, K. Baruch, D. Lara-Astaiso, B. Toth, S. Itzkovitz, M. Colonna, M. Schwartz, I. Amit, A unique microglia type associated with restricting development of Alzheimer's disease. *Cell* **169**, 1276–1290.e17 (2017).
32. S. Parhizkar, D. M. Holtzman, APOE mediated neuroinflammation and neurodegeneration in Alzheimer's disease. *Semin. Immunol.* **59**, 101594 (2022).
33. T. Jonsson, H. Stefansson, S. Steinberg, I. Jonsdottir, P. V. Jonsson, J. Snaedal, S. Bjornsson, J. Huttenlocher, A. I. Levey, J. J. Lah, D. Rujescu, H. Hampel, I. Giegling, O. A. Andreassen, K. Engedal, I. Ulstein, S. Djurovic, C. Ibrahim-Verbaas, A. Hofman, M. A. Ikram, C. M. van Duijn, U. Thorsteinsdottir, A. Kong, K. Stefansson, Variant of TREM2 associated with the risk of Alzheimer's disease. *N. Engl. J. Med.* **368**, 107–116 (2013).
34. R. Guerreiro, A. Wojtas, J. Bras, M. Carrasquillo, E. Rogaeva, E. Majounie, C. Cruchaga, C. Sassi, J. S. K. Kauwe, S. Younkin, L. Hazrati, J. Collinge, J. Pocock, T. Lashley, J. Williams, J.-C. Lambert, P. Amouyel, A. Goate, R. Rademakers, K. Morgan, J. Powell, P. St George-Hyslop, A. Singleton, J. Hardy; Alzheimer Genetic Analysis Group, TREM2 variants in Alzheimer's disease. *N. Engl. J. Med.* **368**, 117–127 (2013).
35. Y. Shi, D. M. Holtzman, Interplay between innate immunity and Alzheimer disease: APOE and TREM2 in the spotlight. *Nat. Rev. Immunol.* **18**, 759–772 (2018).
36. T. R. Jay, V. E. von Saucken, G. E. Landreth, TREM2 in neurodegenerative diseases. *Mol. Neurodegener.* **12**, 56 (2017).
37. S. Krasemann, C. Madore, R. Cialic, C. Baufeld, N. Calcagno, R. El Fatimy, L. Beckers, E. O'Loughlin, Y. Xu, Z. Fanek, D. J. Greco, S. T. Smith, G. Tweet, Z. Humulock, T. Zrzavy, P. Conde-Sanroman, M. Gacias, Z. Weng, H. Chen, E. Tjon, F. Mazaheri, K. Hartmann, A. Madi, J. D. Ulrich, M. Glatzel, A. Worthmann, J. Heeren, B. Budnik, C. Lemere, T. Ikezu, F. L. Heppner, V. Litvak, D. M. Holtzman, H. Lassmann, H. L. Weiner, J. Ochando, C. Haass, O. Butovsky, The TREM2-APOE pathway drives the transcriptional phenotype of dysfunctional microglia in neurodegenerative diseases. *Immunity* **47**, 566–581.e9 (2017).
38. Y. Shi, M. Manis, J. Long, K. Wang, P. M. Sullivan, J. Remolina Serrano, R. Hoyle, D. M. Holtzman, Microglia drive APOE-dependent neurodegeneration in a tauopathy mouse model. *J. Exp. Med.* **216**, 2546–2561 (2019).
39. E. Konijnenberg, B. M. Tijms, J. Gobom, V. Dobricic, I. Bos, S. Vos, M. Tsolaki, F. Verhey, J. Popp, P. Martinez-Lage, R. Vandenberghe, A. Lleo, L. Frolich, S. Lovestone, J. Streffer, L. Bertram, K. Blennow, C. E. Teunissen, R. Veerhuis, A. B. Smit, P. Scheltens, H. Zetterberg, P. J. Visser, APOE ε4 genotype-dependent cerebrospinal fluid proteomic signatures in Alzheimer's disease. *Alzheimers Res. Ther.* **12**, 65 (2020).
40. A. Litvinchuk, T.-P. V. Huynh, Y. Shi, R. J. Jackson, M. B. Finn, M. Manis, C. M. Francis, A. C. Tran, P. M. Sullivan, J. D. Ulrich, B. T. Hyman, T. Cole, D. M. Holtzman, Apolipoprotein E4 reduction with antisense oligonucleotides decreases neurodegeneration in a tauopathy model. *Ann. Neurol.* **89**, 952–966 (2021).
41. C. Wang, M. Xiong, M. Gratuze, X. Bao, Y. Shi, P. S. Andhey, M. Manis, C. Schroeder, Z. Yin, C. Madore, O. Butovsky, M. Artyomov, J. D. Ulrich, D. M. Holtzman, Selective removal of astrocytic APOE4 strongly protects against tau-mediated neurodegeneration and decreases synaptic phagocytosis by microglia. *Neuron* **109**, 1657–1674.e7 (2021).
42. R. Mancuso, G. Fryatt, M. Cleal, J. Obst, E. Pipi, J. Monzón-Sandoval, E. Ribe, L. Winchester, C. Webber, A. Nevado, T. Jacobs, N. Austin, C. Theunis, K. Grauwen, E. Daniela Ruiz, A. Mudher, M. Vicente-Rodriguez, C. A. Parker, C. Simmons, D. Cash, J. Richardson; NIMA Consortium, D. N. C. Jones, S. Lovestone, D. Gómez-Nicola, V. H. Perry, CSF1R inhibitor JNJ-40346527 attenuates microglial proliferation and neurodegeneration in P301S mice. *Brain* **142**, 3243–3264 (2019).
43. C. Geroldi, M. Pihlajamaki, M. P. Laakso, C. DeCarli, A. Beltramello, A. Bianchetti, H. Soininen, M. Trabucchi, G. B. Frisoni, APOE-ε4 is associated with less frontal and more medial temporal lobe atrophy in AD. *Neurology* **53**, 1825–1832 (1999).
44. L. O'Dwyer, F. Lamberton, S. Matura, C. Tanner, M. Scheibe, J. Miller, D. Rujescu, D. Prvulovic, H. Hampel, Reduced hippocampal volume in healthy young ApoE4 carriers: An MRI study. *PLOS ONE* **7**, e48895 (2012).
45. R. de Flores, S. Demeilliez-Servouin, E. Kuhn, L. Chauveau, B. Landeau, N. Delcroix, J. Gonneaud, G. Chételat, Effects of amyloid and *APOE4* on medial temporal lobe subregions in cognitively unimpaired elderly. medRxiv 2022.01. 20.22269607 (2022).
46. M. Donix, A. C. Burggren, N. A. Suthana, P. Siddarth, A. D. Ekstrom, A. K. Krupa, M. Jones, A. Rao, L. Martin-Harris, L. M. Ercoli, K. J. Miller, G. W. Small, S. Y. Bookheimer, Longitudinal changes in medial temporal cortical thickness in normal subjects with the APOE-4 polymorphism. *Neuroimage* **53**, 37–43 (2010).
47. J. Therriault, A. L. Benedet, T. A. Pascoal, S. Mathotaarachchi, M. Chamoun, M. Savard, E. Thomas, M. S. Kang, F. Lussier, C. Tissot, M. Parsons, M. N. I. Qureshi, P. Vitali, G. Massarweh, J. P. Soucy, S. Rej, P. Saha-Chaudhuri, S. Gauthier, P. Rosa-Neto, Association of apolipoprotein E ε4 with medial temporal tau independent of amyloid-β. *JAMA Neurol.* **77**, 470–479 (2020).
48. H. Zetterberg, B. B. Bendlin, Biomarkers for Alzheimer's disease-preparing for a new era of disease-modifying therapies. *Mol. Psychiatry* **26**, 296–308 (2021).
49. K. E. Hopperton, D. Mohammad, M. O. Trepanier, V. Giuliano, R. P. Bazinet, Markers of microglia in post-mortem brain samples from patients with Alzheimer's disease: A systematic review. *Mol. Psychiatry* **23**, 177–198 (2018).
50. S. Venneti, G. Wang, J. Nguyen, C. A. Wiley, The positron emission tomography ligand DAA1106 binds with high affinity to activated microglia in human neurological disorders. *J. Neuropathol. Exp. Neurol.* **67**, 1001–1010 (2008).
51. S. Lavisse, M. Guillermier, A. S. Herard, F. Petit, M. Delahaye, N. Van Camp, L. Ben Haim, V. Lebon, P. Remy, F. Dolle, T. Delzescaux, G. Bonvento, P. Hantraye, C. Escartin, Reactive astrocytes overexpress TSPO and are detected by TSPO positron emission tomography imaging. *J. Neurosci.* **32**, 10809–10818 (2012).
52. M. Pannell, V. Economopoulos, T. C. Wilson, V. Kersemans, P. G. Isenegger, J. R. Larkin, S. Smart, S. Gilchrist, V. Gouverneur, N. R. Sibson, Imaging of translocator protein upregulation is selective for pro-inflammatory polarized astrocytes and microglia. *Glia* **68**, 280–297 (2020).
53. Y. Gui, J. D. Marks, S. Das, B. T. Hyman, A. Serrano-Pozo, Characterization of the 18 kDa translocator protein (TSPO) expression in post-mortem normal and Alzheimer's disease brains. *Brain Pathol.* **30**, 151–164 (2020).
54. S. Palmqvist, N. Mattsson, O. Hansson; Alzheimer's Disease Neuroimaging Initiative, Cerebrospinal fluid analysis detects cerebral amyloid-beta accumulation earlier than positron emission tomography. *Brain* **139**, 1226–1236 (2016).
55. M. Bucci, K. Chiotis, A. Nordberg; Alzheimer's Disease Neuroimaging Initiative, Alzheimer's Disease profiled by fluid and imaging markers: Tau PET best predicts cognitive decline. *Mol. Psychiatry* **26**, 5888–5898 (2021).
56. J. Therriault, E. R. Zimmer, A. L. Benedet, T. A. Pascoal, S. Gauthier, P. Rosa-Neto, Staging of Alzheimer's disease: Past, present, and future perspectives. *Trends Mol. Med.* **28**, 726–741 (2022).
57. R. C. Petersen, Mild cognitive impairment as a diagnostic entity. *J. Intern. Med.* **256**, 183–194 (2004).
58. G. M. McKhann, D. S. Knopman, H. Chertkow, B. T. Hyman, C. R. Jack Jr., C. H. Kawas, W. E. Klunk, W. J. Koroshetz, J. J. Manly, R. Mayeux, R. C. Mohs, J. C. Morris, M. N. Rossor, P. Scheltens, M. C. Carrillo, B. Thies, S. Weintraub, C. H. Phelps, The diagnosis of dementia due to Alzheimer's disease: Recommendations from the National Institute on Aging-Alzheimer's Association workgroups on diagnostic guidelines for Alzheimer's disease. *Alzheimers Dement.* **7**, 263–269 (2011).
59. J. Zou, S. Tao, A. Johnson, Z. Tomljanovic, K. Polly, J. Klein, Q. R. Razlighi, A. M. Brickman, S. Lee, Y. Stern, W. C. Kreisl, Microglial activation, but not tau pathology, is independently associated with amyloid positivity and memory impairment. *Neurobiol. Aging* **85**, 11–21 (2020).
60. T. Terada, M. Yokokura, T. Obi, T. Bunai, E. Yoshikawa, I. Ando, H. Shimada, T. Suhara, M. Higuchi, Y. Ouchi, In vivo direct relation of tau pathology with neuroinflammation in early Alzheimer's disease. *J. Neurol.* **266**, 2186–2196 (2019).
61. S. Bradburn, C. Murgatroyd, N. Ray, Neuroinflammation in mild cognitive impairment and Alzheimer's disease: A meta-analysis. *Ageing Res. Rev.* **50**, 1–8 (2019).
62. A. J. Saykin, L. Shen, X. Yao, S. Kim, K. Nho, S. L. Risacher, V. K. Ramanan, T. M. Foroud, K. M. Faber, N. Sarwar, L. M. Munsie, X. Hu, H. D. Soares, S. G. Potkin, P. M. Thompson, J. S. K. Kauwe, R. Kaddurah-Daouk, R. C. Green, A. W. Toga, M. W. Weiner; Alzheimer's Disease Neuroimaging Initiative, Genetic studies of quantitative MCI and AD phenotypes in ADNI: Progress, opportunities, and plans. *Alzheimers Dement.* **11**, 792–814 (2015).
63. J. P. Ferrari-Souza, P. C. L. Ferreira, B. Bellaver, C. Tissot, Y.-T. Wang, D. T. Leffa, W. S. Brum, A. L. Benedet, N. J. Ashton, M. A. De Bastiani, A. Rocha, J. Therriault, F. Z. Lussier, M. Chamoun, S. Servaes, G. Bezgin, M. S. Kang, J. Stevenson, N. Rahmouni, V. Pallen, N. M. Poltronetti, W. E. Klunk, D. L. Tudorascu, A. Cohen, V. L. Villemagne, S. Gauthier, K. Blennow, H. Zetterberg, D. O. Souza, T. K. Karikari, E. R. Zimmer, P. Rosa-Neto, T. A. Pascoal, Astrocyte biomarker signatures of amyloid-β and tau pathologies in Alzheimer's disease. *Mol. Psychiatry* **27**, 4781–4789 (2022).
64. T. A. Pascoal, M. Shin, M. S. Kang, M. Chamoun, D. Chartrand, S. Mathotaarachchi, I. Bennacef, J. Therriault, K. P. Ng, R. Hopewell, R. Bouhachi, H. H. Hsiao, A. L. Benedet, J. P. Soucy, G. Massarweh, S. Gauthier, P. Rosa-Neto, In vivo quantification of neurofibrillary tangles with [^{18}F]MK-6240. *Alzheimers Res. Ther.* **10**, 74 (2018).
65. Z. Cselényi, M. E. Jönhagen, A. Forsberg, C. Halldin, P. Julin, M. Schou, P. Johnström, K. Varnäs, S. Svensson, L. Farde, Clinical validation of ^{18}F-AZD4694, an amyloid-β–specific PET radioligand. *J. Nucl. Med.* **53**, 415–424 (2012).
66. T. A. Pascoal, J. Therriault, A. L. Benedet, M. Savard, F. Z. Lussier, M. Chamoun, C. Tissot, M. N. I. Qureshi, M. S. Kang, S. Mathotaarachchi, J. Stevenson, R. Hopewell, G. Massarweh, J. P. Soucy, S. Gauthier, P. Rosa-Neto, ^{18}F-MK-6240 PET for early and late detection of neurofibrillary tangles. *Brain* **143**, 2818–2830 (2020).
67. A. Klein, J. Tourville, 101 labeled brain images and a consistent human cortical labeling protocol. *Front. Neurosci.* **6**, 171 (2012).

68. C. R. Jack Jr., H. J. Wiste, S. D. Weigand, T. M. Therneau, V. J. Lowe, D. S. Knopman, J. L. Gunter, M. L. Senjem, D. T. Jones, K. Kantarci, M. M. Machulda, M. M. Mielke, R. O. Roberts, P. Vemuri, D. A. Reyes, R. C. Petersen, Defining imaging biomarker cut points for brain aging and Alzheimer's disease. *Alzheimers Dement.* **13**, 205–216 (2017).
69. M. Schöll, S. N. Lockhart, D. R. Schonhaut, J. P. O'Neil, M. Janabi, R. Ossenkoppele, S. L. Baker, J. W. Vogel, J. Faria, H. D. Schwimmer, G. D. Rabinovici, W. J. Jagust, PET imaging of tau deposition in the aging human brain. *Neuron* **89**, 971–982 (2016).
70. T. A. Pascoal, A. L. Benedet, D. L. Tudorascu, J. Therriault, S. Mathotaarachchi, M. Savard, F. Z. Lussier, C. Tissot, M. Chamoun, M. S. Kang, J. Stevenson, G. Massarweh, M. C. Guiot, J. P. Soucy, S. Gauthier, P. Rosa-Neto, Longitudinal 18F-MK-6240 tau tangles accumulation follows Braak stages. *Brain* **144**, 3517–3528 (2021).
71. T. I. Hansen, V. Brezova, L. Eikenes, A. Haberg, T. R. Vangberg, How does the accuracy of intracranial volume measurements affect normalized brain volumes? Sample size estimates based on 966 subjects from the HUNT MRI cohort. *AJNR Am. J. Neuroradiol.* **36**, 1450–1456 (2015).
72. M. J. Hawrylycz, E. S. Lein, A. L. Guillozet-Bongaarts, E. H. Shen, L. Ng, J. A. Miller, L. N. van de Lagemaat, K. A. Smith, A. Ebbert, Z. L. Riley, C. Abajian, C. F. Beckmann, A. Bernard, D. Bertagnolli, A. F. Boe, P. M. Cartagena, M. M. Chakravarty, M. Chapin, J. Chong, R. A. Dalley, B. D. Daly, C. Dang, S. Datta, N. Dee, T. A. Dolbeare, V. Faber, D. Feng, D. R. Fowler, J. Goldy, B. W. Gregor, Z. Haradon, D. R. Haynor, J. G. Hohmann, S. Horvath, R. E. Howard, A. Jeromin, J. M. Jochim, M. Kinnunen, C. Lau, E. T. Lazarz, C. Lee, T. A. Lemon, L. Li, Y. Li, J. A. Morris, C. C. Overly, P. D. Parker, S. E. Parry, M. Reding, J. J. Royall, J. Schulkin, P. A. Sequeira, C. R. Slaughterbeck, S. C. Smith, A. J. Sodt, S. M. Sunkin, B. E. Swanson, M. P. Vawter, D. Williams, P. Wohnoutka, H. R. Zielke, D. H. Geschwind, P. R. Hof, S. M. Smith, C. Koch, S. G. N. Grant, A. R. Jones, An anatomically comprehensive atlas of the adult human brain transcriptome. *Nature* **489**, 391–399 (2012).
73. G. Gryglewski, R. Seiger, G. M. James, G. M. Godbersen, A. Komorowski, J. Unterholzner, P. Michenthaler, A. Hahn, W. Wadsak, M. Mitterhauser, S. Kasper, R. Lanzenberger, Spatial analysis and high resolution mapping of the human whole-brain transcriptome for integrative analysis in neuroimaging. *Neuroimage* **176**, 259–267 (2018).
74. T. K. Karikari, T. A. Pascoal, N. J. Ashton, S. Janelidze, A. L. Benedet, J. L. Rodriguez, M. Chamoun, M. Savard, M. S. Kang, J. Therriault, M. Schöll, G. Massarweh, J.-P. Soucy, K. Höglund, G. Brinkmalm, N. Mattsson, S. Palmqvist, S. Gauthier, E. Stomrud, H. Zetterberg, O. Hansson, P. Rosa-Neto, K. Blennow, Blood phosphorylated tau 181 as a biomarker for Alzheimer's disease: A diagnostic performance and prediction modelling study using data from four prospective cohorts. *Lancet Neurol.* **19**, 422–433 (2020).
75. J. Lerch, C. Hammill, M. van Eede, D. Cassel, Statistical Tools for Medical Imaging NetCDF (MINC) Files, in R package version 1.5.2.1 (2017); http://mouse-imaging-centre.github.io/RMINC.
76. Y. Rosseel, lavaan: An R Package for Structural Equation Modeling. *J. Stat. Softw.* **48**, 1–36 (2012).
77. R. O. Mueller, G. R. Hancock, Best Practices in Structural Equation Modeling, in *Best Practices in Quantitative Methods*, J. Osborne, Ed. (SAGE, 2008), chap. 32, pp. 488–508.
78. K. Schermelleh-Engel, H. Moosbrugger, H. Müller, Evaluating the fit of structural equation models: Tests of significance and descriptive goodness-of-fit measures. *Meth. Psychol. Res.* **8**, 23–74 (2003).

Acknowledgments: We acknowledge all study participants and the staff of the McGill University Research Center for Studies in Aging. We thank D. Jolly, A. Kostikov, M. Samoila-Lactatus, K. Ross, M. Boudjemeline, and S. Li for assisting in the radiochemistry production, as well as R. Strauss, E. Strauss, G. Gagné, C. Mayhew, T. Vinet-Celluci, K. Wan, S. Sbeiti, M. Jin Joung, M. Olmand, R. Nazar, H.-H. Hsiao, R. Bouhachi, and A. Aliaga for helping with the acquisition of the data. We thank the Colin J. Adair Charitable Foundation. We also acknowledge S. Jones and L. Chouliaras at the University of Cambridge for discussing the findings. The views expressed are those of the authors and not necessarily those of the National Institute for Health Research (NIHR) or the Department of Health and Social Care. **Funding:** This work was supported by Alzheimer's Association (no. AARGD-21-850670, E.R.Z.; nos. NIRG-12-92090 and NIRP-12-259245, P.R.-N.; no. AACSF-20-648075, T.A.P.), Alzheimer's Association and National Academy of Neuropsycology (no. ALZ-NAN-22-928381, E.R.Z.), Brain and Behavioral Research Foundation (no. 29486, D.T.L.), Brain Canada Foundation (CFI project nos. 34874 and 33397, P.R.-N.), Brazilian National Institute of Science and Technology in Excitotoxicity and Neuroprotection (no. 465671/2014-4, E.R.Z.), Canadian Consortium of Neurodegeneration and Aging (no. MOP-11-51-31- team 1, P.R.-N.), Canadian Institutes of Health Research (no. MOP-11-51-31 and nos. RFN 152985, 159815, and 162303, P.R.-N.), CNPq (no. 200691/2021-0, J.P.F.-S.; no. 166407/2020-8, D.T.L.; nos. 312410/2018-2, 435642/2018-9, 312306/2021-0, and 409066/2022-2, E.R.Z.), FAPERGS (no. 21/2551-0000673-0, E.R.Z.), Fonds de Recherche du Québec – Santé (Chercheur Boursier, no. 2020-VICO-279314, P.R.-N.; F.Z.L.), Instituto Serrapilheira (no. Serra-1912-31365, E.R.Z.), Medical Research Council (SUAG/092 116768, J.B.R.), National Institutes of Health (nos. R01AG075336 and R01AG073267, T.A.P.), NIHR Cambridge Biomedical Research Centre (BRC-1215-20014, J.B.R.), Race Against Dementia Alzheimer's Research UK (no. ARUK-RADF2021A-010, M.M.), and Weston Brain Institute (P.R.-N.). **Author contributions:** Conceptualization: J.P.F.-S., F.Z.L., P.R.-N., and T.A.P. Methodology: J.P.F.-S., F.Z.L., and T.A.P. Formal analysis: J.P.F.-S., F.Z.L., C.T., and D.L.T. Investigation: J.P.F.-S., F.Z.L., D.T.L., J.T., C.T., B.B., P.C.L.F., M.M., Y.-T.W., G.P., A.L.B., N.J.A., M.C., S.S., G.B., M.S.K., J.S., N.R., V.P., N.M.P., T.K.K., E.R.Z., P.R.-N., and T.A.P. Resources: H.Z., K.B., and P.R.-N. Writing—original draft: J.P.F.-S. Writing—review and editing: J.P.F.-S., F.Z.L., D.T.L., J.T., C.T., B.B., P.C.L.F., M.M., G.P., A.L.B., N.J.A., J.T.O., J.B.R., A.D.C., O.L.L., D.L.T., T.K.K., W.E.K., V.L.V., J.-P.S., S.G., D.O.S., H.Z., K.B., E.R.Z., P.R.-N., and T.A.P. Supervision: T.A.P. Project administration: J.P.F.-S., P.R.-N., and T.A.P. Funding acquisition: J.P.F.-S., P.R.-N., and T.A.P. **Competing interests:** J.B.R. provides consultancy for Alzheimer's Research UK, Astex, Asceneuron, ICG, SVHealth, Biogen, WAVE, Prevail, and UCB, all unrelated to the present work. S.G. has served as a scientific advisor to Cerveau Therapeutics and has done consulting activities for AmyriAD, Cerveau, Roche, and TauRx. H.Z. has served at scientific advisory boards and/or as a consultant for Abbvie, Alector, Annexon, Apellis, Artery Therapeutics, AZTherapies, CogRx, Denali, Eisai, Nervgen, Novo Nordisk, Pinteon Therapeutics, Red Abbey Labs, reMYND, Passage Bio, Roche, Samumed, Siemens Healthineers, Triplet Therapeutics, and Wave; has given lectures in symposia sponsored by Cellectricon, Fujirebio, Alzecure, Biogen, and Roche; and is a cofounder of Brain Biomarker Solutions in Gothenburg AB (BBS), which is a part of the GU Ventures Incubator Program. K.B. has served as a consultant at advisory boards or at data monitoring committees for Abcam, Axon, BioArctic, Biogen, JOMDD/Shimadzu, Julius Clinical, Lilly, MagQu, Novartis, Prothena, Roche Diagnostics, and Siemens Healthineers; and is a cofounder of Brain Biomarker Solutions in Gothenburg AB (BBS), which is a part of the GU Ventures Incubator Program. E.R.Z. serves in the scientific advisory board of Next Innovative Therapeutics (Nintx). All other authors declare that they have no competing interests. **Data and materials availability:** All data needed to evaluate the conclusions in the paper are present in the paper and/or the Supplementary Materials. The data used in the present work can be provided by the study's senior authors' pending scientific review and a completed material transfer agreement. Requests for data should be submitted to P.R.-N. The data used are not publicly available as the information could compromise the participants' privacy.

Submitted 27 July 2022
Accepted 2 March 2023
Published 5 April 2023
10.1126/sciadv.ade1474